

Superradiant Instability of Near Extremal and Extremal Four-Dimensional Charged Hairy Black Hole in anti-de Sitter Spacetime

P. A. González,^{1,*} Eleftherios Papantonopoulos,^{2,†} Joel Saavedra,^{3,‡} and Yerko Vásquez^{4,§}

¹*Facultad de Ingeniería y Ciencias, Universidad Diego Portales,
Avenida Ejército Libertador 441, Casilla 298-V, Santiago, Chile.*

²*Department of Physics, National Technical University of Athens, Zografou Campus GR 157 73, Athens, Greece.*

³*Instituto de Física, Pontificia Universidad Católica de Valparaíso, Casilla 4950, Valparaíso, Chile.*

⁴*Departamento de Física, Facultad de Ciencias, Universidad de La Serena,
Avenida Cisternas 1200, La Serena, Chile.*

(Dated: March 9, 2017)

We study the instability of near extremal and extremal four-dimensional AdS charged hairy black hole to radial neutral massive and charged massless scalar field perturbations. We solve the scalar field equation by using the improved asymptotic iteration method and the time domain analysis and we find the quasinormal frequencies. For the charged scalar perturbations, we find the superradiance condition by computing the reflection coefficient in the low-frequency limit and we show that in the superradiance regime, which depends on the scalar hair charge, all modes of radial charged massless perturbations are unstable, indicating that the charged hairy black hole is superradiantly unstable. On the other hand, calculating the quasinormal frequencies of radial neutral scalar perturbations in this background, we found stability of the charged hairy black hole.

PACS numbers:

Contents

I. Introduction	1
II. Four-Dimensional Charged Hairy Black Hole	3
III. Scalar perturbations	5
1. Calculation of QNFs using the improved AIM	7
2. Calculation of QNFs using the time domain analysis	10
IV. Superradiant effect	15
V. Conclusions	18
Acknowledgments	18
A. Improved AIM	18
References	19

I. INTRODUCTION

In Gravity theories the stability of black holes has been a central issue and it has been studied for a long time starting from the pioneering work by Regge and Wheeler [1]. It has been found that most of black holes are stable under various types of perturbations. An effective way to study the stability of black holes is to calculate the quasinormal modes (QNMs) and their quasinormal frequencies (QNFs) [2–5]. The QNMs and QNFs give information about the

*Electronic address: pablo.gonzalez@udp.cl

†Electronic address: lpapa@central.ntua.gr

‡Electronic address: joel.saavedra@ucv.cl

§Electronic address: yvasquez@userena.cl

stability of matter fields that evolve perturbatively in the exterior region of a black hole without backreacting on the metric but they carry the information of the black hole because they depend only on their parameters (mass, charge and angular momentum) and the fundamental constants (Newton constant and cosmological constant) of their spacetime, just like the parameters that define the test field. The QNFs have been calculated by means of numerical and analytical techniques. Some well known numerical methods are: the Mashhoon method, Chandrasekhar-Detweiler method, WKB method, Frobenius method, method of continued fractions, Nollert asymptotic iteration method (AIM) and improved AIM, among others (for reviews on QNMs and their QNFs see [6, 7]).

Extensive study of QNMs of black holes in asymptotically flat spacetimes have been performed for the last few decades mainly due to the potential astrophysical interest. Considering the case when the black hole is immersed in an expanding universe, the QNMs of black holes in de Sitter space have also been investigated [8, 9]. The holographic understanding of various system using the AdS/CFT correspondence has triggered recently the study of QNMs in anti-de Sitter (AdS) spacetimes. The first study of the QNMs in AdS spaces was performed in [10]. Subsequently, in [11] it was suggested a numerical method to calculate the QNFs directly and made a systematic investigation of QNMs for scalar perturbation on the background of Schwarzschild-AdS black holes. Later the numerical method of [11] was generalized to the study of QNMs of Reissner-Nordström-AdS black holes in [12]. Also this method was also generalized and extended using the time domain analysis approach [13].

The application of gauge/gravity duality to condense matter systems put forward the necessity to study the behaviour of scalar fields just outside the black hole horizon [14, 15]. The simplest understanding of this application is the holographic superconductor [16]. According to the duality principle, a scalar field minimally coupled to gravity, below a critical temperature condenses outside the black hole horizon, destabilizing the black hole spacetime, and the black hole acquires scalar hair. This mechanism also works if the scalar field is not minimally coupled to gravity [17]. Another interesting application of the gauge/gravity duality is to look on condensed matter systems at criticality where quantum properties of these systems at zero temperature can be studied [18]. The gravity part of these systems is described by an extremal charged black hole in anti-de Sitter spacetime [19]. The metric of the extremal black hole has interesting properties. In the near horizon limit when the temperature goes to zero the horizon geometry is given by $\text{AdS}_2 \times R^2$. In connection to holographic superconductors the near horizon geometry of an extremal black hole was studied in [20].

The above discussion suggests that it is important to study the stability of charged AdS black holes in the presence of scalar hair as the temperature approaches zero. This requires the calculation of the QNMs and QNFs of near extremal and extremal black holes in AdS spacetimes. However, the method developed in [11] breaks down for large values of the charge of the Reissner-Nordström-AdS black holes [12, 13, 21, 22]. Therefore, for large black holes to calculate the QNMs and QNFs of extremal black holes we have to use other methods, like the time domain analysis.

Going to zero temperature at the extremal limit we have also to deal with the applicability of the known methods. In most of the methods calculating the QNMs, a perturbative expansion around the event horizon of the black hole was used. However, the event horizon of an extremal black hole is an irregular singular point of the perturbation equation. Therefore, unlike the case of non-extremal black holes, one does not expect a non-zero radius of convergence of the associated power series around the event horizon. A solution to this problem was proposed in [23] in which an expansion was carried out around an ordinary point of the differential equation. More recently in [24], the modified version of the continued fraction method of [23] was used and the QNMs of charged massless perturbations around an extremal Reissner-Nordström black hole and of neutral massless perturbations around an extremal Kerr black hole were calculated.

The behaviour of matter fields near the horizon of a charged black hole at the zero temperature limit was studied in [25]. To evade the no-hair theorems and have a healthy behaviour of the scalar field, regular on the horizon and fall off sufficiently fast at large distances, a profile for the scalar field was introduced and a fully backreacted solution of the Einstein-Maxwell-scalar system was found. Also, in [26] charged hairy black holes in non-linear electrodynamics were found. Exact solutions of this system without the electromagnetic field were found in [27]. Hairy black holes and their stability were also studied in [28].

In this work, we study the instability of a near extremal and extremal four-dimensional charged hairy black hole in AdS spacetime using the solution found in [25]. In this background we consider a scalar wave minimally coupled to gravity. Then, studying the radial neutral massive and charged massless scalar wave perturbations, we obtain numerically the QNFs of these perturbations. To solve the scalar field equation we use the improved AIM [29], which is an improved version of the method proposed in [30, 31] and it has been applied successfully in the context of QNMs for different black hole geometries (see for instance [29, 32–41]). To obtain the QNFs of the extremal hairy black hole we use the time domain analysis.

For charged scalar perturbations we calculate the superradiance condition by computing the reflection coefficient in the low-frequency limit. We show that the Bekenstein superradiance condition [42] is modified incorporating the information of the presence of scalar hair in the theory. We find that there is a critical value q_c of the charge of the scalar field above which all the modes of radial charged massless perturbations are unstable, which is related

to the charge of the scalar hair, and we show that in this regime the superradiance condition is satisfied, therefore the charged hairy black hole is superradiantly unstable. By calculating the QNFs of radial neutral massless scalar perturbations we find stability, as expected.

The work is organized as follows. In Section II we give a brief review of the four-dimensional charged hairy black hole found in [25]. In Section III we calculate the QNFs of scalar perturbations numerically, by using the improved AIM method in Section III 1 and the time domain analysis in Section III 2. In Section IV we study the superradiant effect calculating the superradiance condition. Finally, our conclusions are in Section V.

II. FOUR-DIMENSIONAL CHARGED HAIRY BLACK HOLE

In this section we will review the charged hairy black hole solution discussed in [25]. This is a solution of a theory that consists of a scalar field minimally coupled to curvature having a self-interacting potential $V(\phi)$, in the presence of an electromagnetic field. The Einstein-Hilbert action with a negative cosmological constant $\Lambda = -6l^{-2}/\kappa$, where l is the length of the AdS space, which it has been incorporated in the potential as $\Lambda = V(0)$ ($V(0) < 0$), reads

$$S = \int d^4x \sqrt{-g} \left(\frac{1}{2\kappa} R - \frac{1}{4} F_{\mu\nu} F^{\mu\nu} - \frac{1}{2} g^{\mu\nu} \nabla_\mu \phi \nabla_\nu \phi - V(\phi) \right), \quad (2.1)$$

where $\kappa = 8\pi G_N$, with G_N the Newton constant. The resulting Einstein equations from the above action are

$$R_{\mu\nu} - \frac{1}{2} g_{\mu\nu} R = \kappa (T_{\mu\nu}^{(\phi)} + T_{\mu\nu}^{(F)}), \quad (2.2)$$

where the energy momentum tensors $T_{\mu\nu}^{(\phi)}$ and $T_{\mu\nu}^{(F)}$ for the scalar and electromagnetic fields are

$$\begin{aligned} T_{\mu\nu}^{(\phi)} &= \nabla_\mu \phi \nabla_\nu \phi - g_{\mu\nu} \left[\frac{1}{2} g^{\rho\sigma} \nabla_\rho \phi \nabla_\sigma \phi + V(\phi) \right], \\ T_{\mu\nu}^{(F)} &= F_\mu^\alpha F_{\nu\alpha} - \frac{1}{4} g_{\mu\nu} F_{\alpha\beta} F^{\alpha\beta}. \end{aligned} \quad (2.3)$$

If we use Eqs. (2.2) and (2.3) we obtain the equivalent equation

$$R_{\mu\nu} - \kappa (\partial_\mu \phi \partial_\nu \phi + g_{\mu\nu} V(\phi)) = \kappa (F_\mu^\alpha F_{\nu\alpha} - \frac{1}{4} g_{\mu\nu} F_{\alpha\beta} F^{\alpha\beta}). \quad (2.4)$$

We consider the following metric ansatz

$$ds^2 = -f(r) dt^2 + f^{-1}(r) dr^2 + a^2(r) d\sigma^2, \quad (2.5)$$

where $d\sigma^2$ is the metric of the spatial 2-section, which can have positive, negative or zero curvature, and $A_\mu = (A_t(r), 0, 0, 0)$ the scalar potential of the electromagnetic field.

A particular profile of the scalar field was considered in [25]

$$\phi(r) = \frac{1}{\sqrt{2}} \ln \left(1 + \frac{\nu}{r} \right), \quad (2.6)$$

where ν is the scalar charge, a parameter controlling the behaviour of the scalar field and it has the dimension of length and then the following analytical solution was found

$$\begin{aligned} a(r) &= \sqrt{r(r+\nu)}, \\ A_t(r) &= \frac{Q}{\nu} \ln \left(\frac{r}{r+\nu} \right). \end{aligned} \quad (2.7)$$

The metric function $f(r)$ is

$$\begin{aligned} f(r) &= -2 \frac{Q^2}{\nu^2} + C_1 r(r+\nu) - \frac{C_2(2r+\nu)}{\nu^2} + 2 \frac{kr(2r+\nu)}{\nu^2} \\ &\quad - 2 \left(\frac{Q^2(2r+\nu) + r(r+\nu)(C_2 + k\nu)}{\nu^3} + \frac{Q^2 r(r+\nu) \ln \frac{r}{r+\nu}}{\nu^4} \right) \ln \frac{r}{r+\nu}, \end{aligned} \quad (2.8)$$

where $k = -1, 0, 1$ parameterizes the curvature of the transverse 2-section and C_1, C_2 are integration constants being proportional to the cosmological constant and to the mass respectively, and the potential is given by

$$\begin{aligned}
V(\phi) = & \frac{1}{2\nu^4} e^{-2\sqrt{2}\phi} \left(\left(e^{-2\sqrt{2}\phi} - 1 \right)^2 \left(1 + 10e^{\sqrt{2}\phi} + e^{\sqrt{2}\phi} \right) Q^2 \right. \\
& + e^{\sqrt{2}\phi} \nu \left(-6C_2 - 10k\nu - C_1\nu^3 - 4e^{\sqrt{2}\phi} \nu (4k + C_1\nu^2) + e^{2\sqrt{2}\phi} (6C_2 + 2k\nu - C_1\nu^3) \right) \\
& + 2\coth\frac{\phi}{\sqrt{2}} \left(\left(1 + 4e^{\sqrt{2}\phi} + e^{2\sqrt{2}\phi} \right) Q^2 \ln \frac{\nu}{-1 + e^{\sqrt{2}\phi}} \right. \\
& \left. \left. \left. 2e^{\sqrt{2}\phi} \left(\left(2 + \cosh\sqrt{2}\phi \right) \left(\nu(C_2 + k\nu) + Q^2 \ln(1 - e^{\sqrt{2}\phi}) + 6Q^2 \sinh\sqrt{2}\phi \right) \right) \right) \right), \tag{2.9}
\end{aligned}$$

where $V(0) = \Lambda_{eff}$ as expected and also

$$C_1 + \frac{4k}{\nu^2} = -\frac{\Lambda_{eff}}{3} = \frac{1}{l^2}. \tag{2.10}$$

We see from the above relation that the parameter ν of the scalar field introduces a length scale connected with the presence of the scalar field in the theory. Besides, we know that

$$V''(\phi=0) = m^2, \tag{2.11}$$

where m is the scalar field mass. Therefore, we obtain that the scalar field mass is given by

$$m^2 = \frac{2}{3} \Lambda_{eff} = -2l^{-2}, \tag{2.12}$$

which satisfies the Breitenlohner-Friedman bound that ensures the perturbative stability of the AdS spacetime [43].

One may wonder if in the limit of $\Lambda_{eff} \rightarrow 0$ and $\nu \rightarrow 0$ we recover the Reissner-Nordström (RN) black hole. Indeed from (2.8) if we fix the constant C_1 to $C_1 = -\frac{4k}{\nu^2}$ the function $f(r)$ can be written as

$$\begin{aligned}
f(r) = & -\frac{2(Q^2 + 5\nu + r(C_2 + k\nu))}{\nu^2} \\
& -\frac{2\left(\nu(Q^2(2r + \nu) + r(r + \nu)(C_2 + k\nu)) + Q^2 r(r + \nu) \ln \frac{r}{r+\nu}\right) \ln \frac{r}{r+\nu}}{\nu^4}, \tag{2.13}
\end{aligned}$$

and in the limit $\nu \rightarrow 0$ we recover the RN black hole

$$f(r) = k + \frac{Q^2}{2r^2} - \frac{C_2}{3r}. \tag{2.14}$$

It was shown, that in the case of $\Lambda_{eff} = 0$ at all temperature the RN black hole solution is thermodynamically preferred over the charged hairy black hole solution. In the case of $\Lambda_{eff} \neq 0$ the charged hairy black hole is thermodynamically preferred over the RN black hole at low temperature. This picture is in agreement with the findings of the application of the AdS/CFT correspondence to condensed matter systems. In these systems there is a critical temperature below which the system undergoes a phase transition to a hairy black hole configuration at low temperature. This corresponds in the boundary field theory to the formation of a condensation of the scalar field [16, 44]. On the other hand, classically, it was shown that there are bounded orbits like planetary orbits in this background. Also, the periods associated to circular orbits are modified by the presence of the scalar hair. Besides, some classical tests such as perihelion precession, deflection of light and gravitational time delay have the standard value of general relativity plus a correction term coming from the cosmological constant and the scalar hair. Furthermore, it is possible to find a specific value of the parameter associated to the scalar hair, in order to explain the discrepancy between the theory and the observations, for the perihelion precession of Mercury and light deflection [45].

Now, we make the following redefinitions

$$\begin{aligned}
C_1 &= -\frac{\Lambda}{3} - \frac{4k}{\nu^2}, \\
C_2 &= \alpha_2 \nu^3 - k\nu, \\
Q^2 &= \alpha_1 \nu^4. \tag{2.15}
\end{aligned}$$

Then the potential becomes

$$\begin{aligned}
V(\phi) = & \alpha_1(8\phi^2 + 4(\phi^2 + 2)\cosh(\sqrt{2}\phi) - 12\sqrt{2}\phi\sinh(\sqrt{2}\phi) + \cosh(2\sqrt{2}\phi) - 9) \\
& + 6\alpha_2\sinh(\sqrt{2}\phi) - 2\sqrt{2}\alpha_2\phi(\cosh(\sqrt{2}\phi) + 2) + \frac{1}{3}\Lambda(\cosh(\sqrt{2}\phi) + 2),
\end{aligned} \tag{2.16}$$

while the metric function is

$$\begin{aligned}
f(r) = & -\frac{\Lambda r^2}{3} - \left(\frac{\Lambda}{3} + 2\alpha_2\right)\nu r - (2\alpha_1 + \alpha_2)\nu^2 + k \\
& - 2(\alpha_1\nu^2 + \alpha_2r^2 + \nu r(2\alpha_1 + \alpha_2))\ln\left(\frac{r}{r+\nu}\right) - 2\alpha_1r(r+\nu)\ln^2\left(\frac{r}{r+\nu}\right).
\end{aligned} \tag{2.17}$$

The scalar field is

$$\phi = \frac{1}{\sqrt{2}}\ln\left(1 + \frac{\nu}{r}\right), \tag{2.18}$$

and the electric potential becomes

$$A_t = \sqrt{\alpha_1}\nu\ln\left(\frac{r}{r+\nu}\right). \tag{2.19}$$

With this redefinition the solution has one integration constant ν (the electric charge is not independent) and the self interaction potential has three parameters, the cosmological constant Λ and two coupling constants α_1 and α_2 .

III. SCALAR PERTURBATIONS

The QNMs of charged scalar perturbations in the background of the metric (2.17) are given by the scalar field solution of the Klein-Gordon equation

$$\frac{1}{\sqrt{-g}}(\partial_\mu - iqA_\mu)(\sqrt{-g}g^{\mu\nu}(\partial_\nu - iqA_\nu)\varphi) = m^2\varphi, \tag{3.1}$$

with suitable boundary conditions for a black hole geometry. In the above expression m is the mass and q is the electric charge of the scalar field φ . In the following we will focus our attention to spherical transverse section ($k = 1$). Now, by means of the following ansatz

$$\varphi = e^{-i\omega t}R(r)Y(\Omega), \tag{3.2}$$

the Klein-Gordon equation reduces to

$$\frac{d}{dr}\left(a(r)^2f(r)\frac{dR}{dr}\right) + \left(\frac{a(r)^2(\omega + qA_t(r))^2}{f(r)} - \kappa^2 - m^2a(r)^2\right)R(r) = 0, \tag{3.3}$$

where we have defined $-\kappa^2 = -\ell(\ell + 1)$, with $\ell = 0, 1, 2, \dots$, which represents the eigenvalue of the Laplacian on the two-sphere. Now, defining the radial function $R(r)$ as

$$R(r) = \frac{F(r)}{a(r)}, \tag{3.4}$$

and by using the tortoise coordinate r^* given by

$$dr^* = \frac{dr}{f(r)}, \tag{3.5}$$

the Klein-Gordon equation can be written as a one-dimensional Schrödinger equation

$$\frac{d^2F(r^*)}{dr^{*2}} - V_{eff}(r)F(r^*) = -\omega^2F(r^*), \tag{3.6}$$

with an effective potential $V_{eff}(r)$, which is parametrically written as $V_{eff}(r^*)$ and it is given by

$$V_{eff}(r) = \frac{f(r)}{a(r)^2} (\kappa^2 + a(r) (m^2 a(r) + a'(r)f'(r) + a''(r)f(r))) - 2q\omega A_t(r) - q^2 A_t(r)^2. \quad (3.7)$$

For neutral scalar field $q = 0$, the effective potential is real and diverges at spatial infinity. In Fig. 1 we plot the lapsus function and in Fig. 2 the potential, where we have considered a spherical transverse section ($k = 1$), massive scalar fields with $m = 0.1$, $\alpha_1 = 1$, $\alpha_2 = 2$, $\Lambda = -0.1$, $\kappa = 0$, and $\nu = 3.5, 3.0, 2.512$, for $\nu \approx 2.5119365 \approx 2.512$ the black hole is extremal and then we choose different values of ν in order to consider near extremal black holes. The event horizon for the extremal black hole is localized at $r_+ \approx 2.0921064 \approx 2.09$.

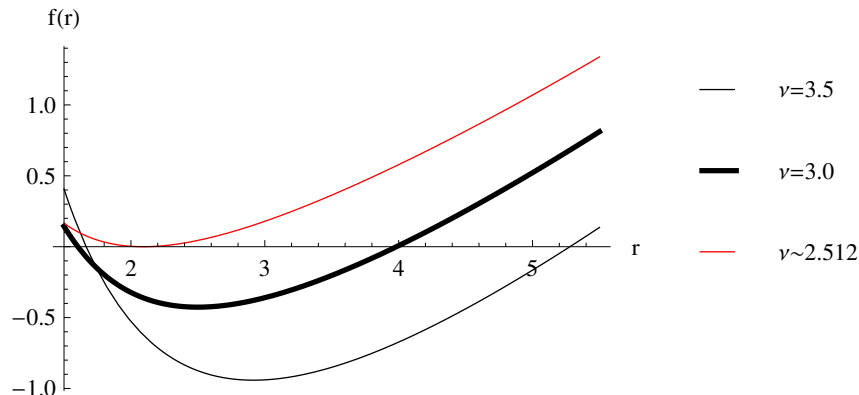


FIG. 1: The behavior of $f(r)$ with $\alpha_1 = 1$, $\alpha_2 = 2$, $m = 0.1$, $q = 0$, $k = 1$, $\kappa = 0$, and $\Lambda = -0.1$.

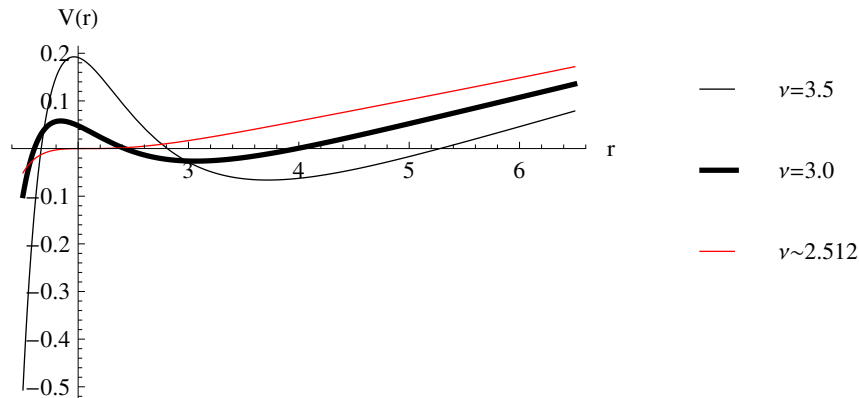


FIG. 2: The behavior of $V_{eff}(r)$ with $\alpha_1 = 1$, $\alpha_2 = 2$, $m = 0.1$, $q = 0$, $k = 1$, $\kappa = 0$, and $\Lambda = -0.1$.

In order to know about the stability of scalar fields in the background of a black hole, we follow a general argument given in Ref. [11]. So, by defining

$$\psi(r) = e^{i\omega r^*} F(r), \quad (3.8)$$

and inserting this expression in the Schrodinger like equation (3.6) yields

$$\frac{d}{dr} \left(f(r) \frac{d\psi(r)}{dr} \right) - 2i\omega \frac{d\psi(r)}{dr} - \frac{V_{eff}(r)}{f(r)} \psi(r) = 0. \quad (3.9)$$

Then, multiplying Eq. (3.9) by ψ^* and performing integrations by parts, and additionally using the Dirichlet boundary condition for the scalar field at spatial infinity, one can obtain the following expression

$$\int_{r_+}^{\infty} dr \left(f(r) \left| \frac{d\psi}{dr} \right|^2 + \frac{V_{eff}(r)|_{q=0}}{f(r)} |\psi|^2 - \frac{q^2 A_t(r)^2}{f(r)} |\psi|^2 \right) = - \frac{|\omega|^2 |\psi(r=r_h)|^2}{\text{Im}(\omega)}. \quad (3.10)$$

In general, the QNFs are complex, where the real part represents the oscillation frequency and the imaginary part describes the rate at which this oscillation is damped, with the stability of the scalar field being guaranteed if the imaginary part is negative. Notice that the sign outside the horizon of the expression $V_{eff}|_{q=0} - q^2 A_t^2$, which appears inside the integral of the above equation, is crucial for stability. For the neutral scalar perturbations the effective potential (3.7) is positive outside the horizon and then the left hand side of (3.10) is strictly positive, which demand that $Im(\omega) < 0$, and then we conclude that the stability of the neutral scalar field under perturbations respecting Dirichlet boundary conditions is obeyed. For charged scalar field, the integral can yield a negative value, therefore the stability is not guaranteed in this case.

In the following we will compute numerically the QNFs by using the improved AIM for hairy black hole. However, as we discussed in the introduction the improved AIM breaks down when we approach the extremal limit. Therefore, we will use the time domain analysis to compute numerically the QNFs in this limit.

1. Calculation of QNFs using the improved AIM

Now, in order to implement the improved AIM (we give a brief review of the improved AIM in the Appendix) we perform the change of variable $y = 1 - \frac{r_{\pm}}{r}$. So, the Klein-Gordon equation reads

$$R''(y) + \left(2 \frac{a'(y)}{a(y)} + \frac{f'(y)}{f(y)} - \frac{2}{1-y} \right) R'(y) + \frac{r_+^2}{(1-y)^4} \left(\frac{(\omega + qA_t(y))^2}{f(y)^2} - \frac{\kappa^2}{a(y)^2 f(y)} - \frac{m^2}{f(y)} \right) R(y) = 0. \quad (3.11)$$

In this equation the functions $f(y)$, $a(y)$ and $A_t(y)$ refers to the functions $f(r)$, $a(r)$ and $A_t(r)$ evaluated at $r = \frac{r_{\pm}}{1-y}$, and we will study the behaviour of the above equation at the horizon and at spatial infinite. At the event horizon $y = 0$, the Eq. (3.11) can be written as

$$R''(y) + \frac{1}{y} R'(y) + \frac{r_+^2 (\omega + qA_t(0))^2}{f'(0)^2 y^2} R(y) = 0, \quad (3.12)$$

where we have considered the Taylor expansion of the lapse function around the event horizon $f(y) \approx f'(0)y + \mathcal{O}(y^2)$. Then, the solution is given by

$$R(y) = C_1 e^{\frac{ir_+(\omega + qA_t(0)) \ln y}{f'(0)}} + C_2 e^{-\frac{ir_+(\omega + qA_t(0)) \ln y}{f'(0)}}, \quad (3.13)$$

which it can be written in terms of the tortoise coordinate r^* , and near the horizon is given by $r^* = \frac{r_+}{f'(0)} \ln y$, as

$$R(y) = C_1 e^{i(\omega + qA_t(0))r^*} + C_2 e^{-i(\omega + qA_t(0))r^*}. \quad (3.14)$$

So, by imposing as a boundary condition that only ingoing waves exist on the event horizon, we must set $C_1 = 0$. Therefore, the solution near the horizon is given by

$$R(y) = C_2 e^{-\frac{ir_+(\omega + qA_t(0)) \ln y}{f'(0)}} = C_2 y^{-\frac{ir_+(\omega + qA_t(0))}{f'(0)}}. \quad (3.15)$$

On the other hand, at spatial infinity, the Klein-Gordon equation becomes

$$R''(y) + \frac{2}{1-y} R'(y) + \frac{3m^2}{\Lambda(1-y)^2} R(y) = 0, \quad (3.16)$$

whose solution is

$$R(y) = D_1 (1-y)^{\beta_+} + D_2 r (1-y)^{\beta_-}, \quad (3.17)$$

where $\beta_{\pm} = \frac{3}{2} \pm \sqrt{\left(\frac{3}{2}\right)^2 - \frac{3m^2}{\Lambda}}$. So, imposing the Dirichlet boundary condition; that is, having a null scalar field at spatial infinity, we must set $D_2 = 0$. Therefore, in order to implement the above boundary conditions in the improved AIM, we must redefine the radial function $R(y)$ in terms of a new function, say $\chi(y)$, in the following form

$$R(y) = y^{\alpha} (1-y)^{\beta} \chi(y), \quad (3.18)$$

where

$$\alpha = -\frac{ir_+(\omega + qA_t(0))}{f'(0)},$$

$$\beta = \frac{3}{2} + \sqrt{\left(\frac{3}{2}\right)^2 - \frac{3m^2}{\Lambda}}.$$

Then, by inserting the above expression for $R(y)$ in Eq. (3.11), we obtain the following homogeneous linear second-order differential equation for the function $\chi(y)$

$$\chi''(y) = \lambda_0(y)\chi'(y) + s_0(y)\chi(y), \quad (3.19)$$

where

$$\lambda_0(y) = -\frac{2f(y)((y-1)ya'(y) + a(y)(y(\alpha + \beta + 1) - \alpha)) + (y-1)ya(y)f'(y)}{(y-1)ya(y)f(y)}, \quad (3.20)$$

$$s_0(y) = -\frac{\beta(\beta+1)y^2 + \alpha^2(y-1)^2 + \alpha(y-1)(2\beta y + y + 1)}{(y-1)^2y^2} - \frac{2(y-1)^3a(y)f(y)a'(y)(\alpha(y-1) + \beta y) - \kappa^2r_+^2y}{(y-1)^4ya(y)^2f(y)} \quad (3.21)$$

$$-\frac{r_+^2y((\omega + qA_t(y))^2 - m^2f(y)) + (y-1)^3f(y)f'(y)(\alpha(y-1) + \beta y)}{(y-1)^4yf(y)^2}. \quad (3.22)$$

We solve this equation numerically and we choose different values for the parameter ν such that the difference between the roots of the lapsus function $\Delta r = r_+ - r_-$ decreases. Then, in Table I we show the fundamental QNFs for neutral massive scalar fields in the background of a hairy black hole with $\kappa = 0$, $\alpha_1 = 1$, $\alpha_2 = 2$, $k = 1$ and different values of m and ν and we plot these values in Fig. 3. Furthermore, we observe that in all the cases analyzed the QNFs have an imaginary part that is negative. So, we conclude that the radial massive neutral scalar field perturbations are stable in the hairy black hole background and the system is always overdamped, that is, the QNFs have no real part so there is no oscillatory behaviour in the perturbations, only exponential decay.

Also, for all cases analyzed, when we approach to the extremal limit ($\nu \approx 2.512$), the absolute value of imaginary part decreases, see Fig. 3, which means that the damping time $\tau = 1/\omega_I$, where ω_I is the imaginary part of QNFs, is increasing. This result is interesting because it may have applications to the thermalization process of a quark-gluon plasma according to the gauge/gravity duality. The recent theoretical and experimental developments indicate that the quark-gluon plasma produced at Relativistic Hadron Ion Collider is a strongly interacting liquid and the produced plasma locally isotropizes over a time scale of $\tau_{iso} < \frac{1fm}{c}$. The dynamics of such isotropization in a far-from-equilibrium non-Abelian plasma cannot be described with the standard methods of field theory or hydrodynamics. Then it was proposed in [46, 47] that such a thermalization can be studied via its gravity dual identifying τ with the thermalization time.

Besides, when the mass of the scalar field increases the absolute value of imaginary part increases and consequently the relaxation time decreases. It is worth mentioning, that in Table I, we were able to compute the QNFs until $\Delta r \approx 0.3$, for smaller values is difficult to find the QNFs by using the improved AIM. However, in the next section we will reach smaller values of Δr for the near extremal black hole and the extremal black hole by using the time domain analysis.

On the other hand, for $\kappa = 0$, $\alpha_1 = 1$, $\alpha_2 = 2$, $\Lambda = -0.1$, $m = 0$, $k = 1$ and radial massless charged scalar perturbations we give the fundamental QNFs in Table II and Table III for various values of q and ν and we plot in the complex plane some of these values in Fig. 4. We observe that the QNFs present a real and imaginary part for massless charged scalar perturbations. Also, for most of cases analyzed, when we approach to the extremal case, the value of real part decreases. Besides, we observe that as the charge q is increasing more QNFs with positive imaginary part appear indicating an instability of the near extremal hairy black hole under radial massless charged perturbations. This behaviour can be seen clearly in Fig. 4. In the next section we will show that these instabilities are due to the superradiant effect.

Furthermore, in Table IV we obtain the relation between q and ν for which the QNFs are purely real, for $\kappa = 0$, $\alpha_1 = 1$, $\alpha_2 = 2$, $\Lambda = -0.1$, $m = 0$, $k = 1$, and in Fig. 5 we depict the values of Table IV, i.e. q as a function of ν . We observe that for values of q above the curve, the modes are unstable, while for values of q below the curve, the modes are stable. Note that the values of q , ν and ω given in Table IV satisfy the condition $\omega = q\sqrt{\alpha_1\nu} \log(1 + \nu/r_+)$, which

TABLE I: Fundamental quasinormal frequencies for radial neutral scalar fields in the background of the charged hairy black hole with $\kappa = 0$, $\alpha_1 = 1$, $\alpha_2 = 2$, $\Lambda = -0.1$, $q = 0$, $k = 1$ and different values of m and ν .

ν	Δr	$m = 0$	$m = 0.1$	$m = 0.5$	$m = 1$
5.50	7.48	$-1.29298i$	$-1.31062i$	$-1.74474i$	$-2.61162i$
5.00	6.59	$-1.13103i$	$-1.14816i$	$-1.53897i$	$-2.30644i$
4.50	5.66	$-0.96483i$	$-0.98117i$	$-1.32610i$	$-1.99059i$
4.00	4.68	$-0.79231i$	$-0.80735i$	$-1.10221i$	$-1.65809i$
3.50	3.61	$-0.60870i$	$-0.62168i$	$-0.85916i$	$-1.29637i$
3.00	2.38	$-0.39963i$	$-0.40917i$	$-0.57411i$	$-0.87034i$
2.75	1.60	$-0.26807i$	$-0.27485i$	$-0.38946i$	$-0.59271i$
2.70	1.41	$-0.23609i$	$-0.24213i$	$-0.34394i$	$-0.52401i$
2.60	0.95	$-0.15816i$	$-0.16232i$	$-0.23207i$	$-0.35463i$
2.55	0.62	$-0.10248i$	$-0.10524i$	$-0.15129i$	$-0.23179i$
2.53	0.42	$-0.06999i$	$-0.07191i$	$-0.10380i$	$-0.15928i$
2.525	0.36	$-0.05935i$	$-0.06099i$	$-0.08817i$	$-0.13537i$
2.521	0.30	$-0.04929i$	$-0.05066i$	$-0.07336i$	$-0.11270i$

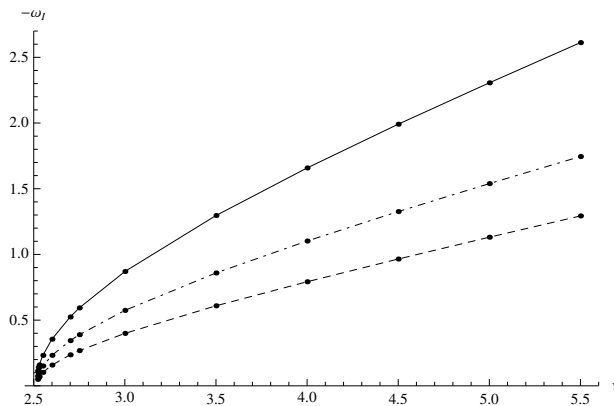


FIG. 3: The behaviour of $-\omega_I$ for $\kappa = 0$, $\alpha_1 = 1$, $\alpha_2 = 2$, $\Lambda = -0.1$, $q = 0$, $k = 1$ and different values of m and ν . $m = 0$ (dashed line), $m = 0.5$ (dot-dashed line) and $m = 1$ (continuous line) .

is closely related to the superradiance condition $\omega < q\sqrt{\alpha_1}\nu \log(1 + \nu/r_+)$ that we will obtain in the next section, and we will show that all the unstable modes are superradiant, while the stable modes are not superradiant. Additionally, the curve in Fig. 5 shows that for a fixed value of q there is a limited value of ν , such that above this limit the modes are stable and under this value the modes are unstable triggering the superradiance instability. Besides, for a fixed value of ν there is a maximum value of q such that under this value the modes are stable and over this value the modes are unstable triggering the superradiance instability.

TABLE II: Fundamental quasinormal frequencies for massless charged scalar fields in the background of the charged hairy black hole with $\kappa = 0$, $\alpha_1 = 1$, $\alpha_2 = 2$, $\Lambda = -0.1$, $m = 0$, $k = 1$ and different values of q and ν .

ν	Δr	$q = 0$	$q = 0.1$	$q = 0.3$	$q = 0.5$	$q = 1$
30	46.58	-8.37759i	3.83217 - 5.73207i	6.55775 - 3.62443i	8.91096 - 2.38963i	14.02910 - 0.61098i
25	38.75	-6.96313i	3.19315 - 4.77281i	5.46656 - 3.01522i	7.42874 - 1.98619i	11.69600 - 0.50530i
20	30.89	-5.54380i	2.55402 - 3.81249i	4.37586 - 2.40459i	5.94733 - 1.58134i	9.36438 - 0.39858i
15	23	-4.11487i	1.91461 - 2.85004i	3.28614 - 1.79113i	4.46756 - 1.17364i	7.03560 - 0.28979i
10	15.01	-2.66288i	1.27414 - 1.88231i	2.19888 - 1.17044i	2.99201 - 0.75873i	4.71419 - 0.17594i
9	3.51	-2.36665i	1.14564 - 1.68736i	1.98209 - 1.04433i	2.69807 - 0.67380i	4.25195 - 0.15187i
8	11.74	-2.06700i	1.01676 - 1.49155i	1.76572 - 0.91697i	2.40489 - 0.58761i	3.79105 - 0.12701i
7	10.07	-1.76270i	0.88716 - 1.29452i	1.54996 - 0.78776i	2.11284 - 0.49962i	3.33213 - 0.10108i
6	8.36	-1.45183i	0.75601 - 1.09567i	1.33511 - 0.65569i	1.82259 - 0.40883i	2.87635 - 0.07367i
5.5	7.48	-1.29298i	0.68917 - 0.99524i	1.22819 - 0.58802i	1.67851 - 0.36186i	2.65028 - 0.05926i
5	6.59	-1.13103i	0.62056 - 0.89381i	1.12174 - 0.51875i	1.53548 - 0.31336i	2.42601 - 0.04431i
4.5	5.66	-0.96483i	0.54830 - 0.79070i	1.01592 - 0.44719i	1.39400 - 0.26273i	2.20431 - 0.02886
4	4.68	-0.79231i	0.46764 - 0.68287i	0.91091 - 0.37218i	1.25490 - 0.20897i	1.98637 - 0.01328i
3.5	3.61	-0.60870i	0.37235 - 0.55477i	0.80689 - 0.29133i	1.11992 - 0.15023i	1.77398 + 0.00100i
3	2.38	-0.39963i	0.27679 - 0.37773i	0.70326 - 0.19800i	0.99369 - 0.08226i	1.56765 + 0.00956i
2.7	1.41	-0.23609i	0.22611 - 0.22627i	0.63818 - 0.12323i	0.92954 - 0.03180i	1.44390 + 0.01063i
2.55	0.62	-0.10248i	0.20318 - 0.09867i	0.60083 - 0.05581i	0.91176 - 0.00084i	1.38163 + 0.01081i
2.52	0.28	-0.04645i	0.19903 - 0.04470i	0.59345 - 0.02435i	0.91306 + 0.00338i	--
2.515	0.17	-0.02848i	0.19842 - 0.02738i	0.59285 - 0.01420i	0.91324 + 0.00355i	--

TABLE III: Fundamental quasinormal frequencies for massless charged scalar fields in the background of the charged hairy black hole with $\kappa = 0$, $\alpha_1 = 1$, $\alpha_2 = 2$, $\Lambda = -0.1$, $m = 0$, $k = 1$ and different values of q and ν .

ν	$q = 1.2$	$q = 1.3$	$q = 1.5$	$q = 2$
30	15.86600 - 0.23512i	16.73990 - 0.10562i	18.38480 + 0.05466i	21.87910 + 0.16806i
25	13.22730 - 0.19309i	13.95560 - 0.08576i	15.32610 + 0.04671i	18.23650 + 0.14024i
20	10.59010 - 0.15031i	11.17280 - 0.06530i	12.26880 + 0.03905i	14.59500 + 0.11248i
15	7.95602 - 0.10605i	8.39322 - 0.04370i	9.21449 + 0.03192i	10.95550 + 0.08481i
10	5.32988 - 0.05834i	5.62154 - 0.01952i	6.16737 + 0.02590i	7.32117 + 0.057382i
9	4.80682 - 0.04796i	5.06934 - 0.01410i	5.55984 + 0.02490i	6.59566 + 0.05195i
8	4.28515 - 0.03713i	4.51848 - 0.00838i	4.95345 + 0.02398i	5.87096 + 0.04656i
7	3.76550 - 0.02574i	3.96956 - 0.00236i	4.34864 + 0.02309i	5.14741 + 0.04121i
6	3.24896 - 0.01373i	3.42351 + 0.00391i	3.74608 + 0.02215i	4.42553 + 0.03592i
5.5	2.99241 - 0.00756i	3.15203 + 0.00703i	3.44593 + 0.02158i	4.06548 + 0.03330i
5	2.73746 - 0.00139i	2.88190 + 0.00997i	3.14675 + 0.02090i	3.70623 + 0.03072i
4.5	2.48458 + 0.00447i	2.61342 + 0.01250i	2.84872 + 0.02004i	3.34802 + 0.02817i
4	2.23426 + 0.00943i	2.34681 + 0.01421i	2.55208 + 0.01898i	2.99117 + 0.02567i
3.5	1.98656 + 0.01245i	2.08202 + 0.01474i	2.25718 + 0.01775i	2.63618 + 0.02322i
3	1.74047 + 0.01307i	1.81894 + 0.01431i	1.96469 + 0.01648i	2.28378 + 0.02085i
2.7	1.59346 + 0.01292i	1.66226 + 0.01392i	1.79080 + 0.01572i	2.07406 + 0.01945i

2. Calculation of QNFs using the time domain analysis

In this section we will apply a time evolution approach [48] in order to compute the QNFs for the near extremal and the extremal hairy black hole, due to the failure of applicability of the improved AIM when we consider the extremal limit. It is worth mentioning that the QNFs for the extremal BTZ black hole cannot be obtained as limits of non-extremal BTZ black holes [49], and the imaginary part of the frequencies is zero (non-dissipative modes). However, this behaviour can be explained because the change of variables in order to find an hypergeometric differential equation for the radial equation for the BTZ black hole, is not well defined when the two horizons coincide. In our case, the

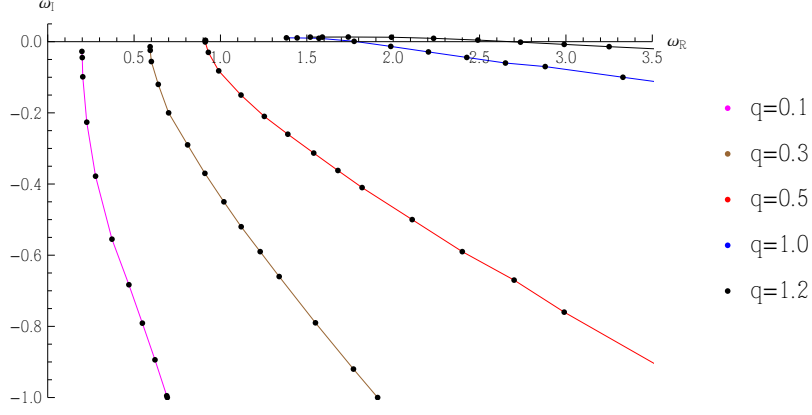


FIG. 4: The behaviour of ω in the complex plane for $\kappa = 0$, $\alpha_1 = 1$, $\alpha_2 = 2$, $\Lambda = -0.1$, $m = 0$, $k = 1$ and different values of q and ν .

TABLE IV: Fundamental quasinormal frequencies for massless charged scalar fields with null imaginary part in the background of the charged hairy black hole with $\kappa = 0$, $\alpha_1 = 1$, $\alpha_2 = 2$, $\Lambda = -0.1$, $m = 0$, $k = 1$ and different values of q .

q	0.5	0.6	0.7	0.8	0.9	1.0	1.1	1.2	1.3	1.35	1.375	1.4
ν	2.54565	2.6248	2.7544	2.93848	3.1902	3.5392	4.05	4.88485	6.6214	8.6802	10.8395	16.318
ω	0.91179	1.04255	1.18262	1.34389	1.53952	1.79039	2.13727	2.67902	3.76242	5.01555	6.31449	9.58243

change of variables that we will perform is well defined for the extremal case. So, first it is convenient to express the metric in terms of the ingoing Eddington-Finkelstein coordinate $v = t + r^*$ [50, 51]

$$ds^2 = -f(r)dv^2 + 2dvdr + a(r)^2 d\sigma^2. \quad (3.23)$$

The electromagnetic potential can be written as

$$A = \sqrt{\alpha_1} \nu \log\left(\frac{r}{r+\nu}\right) dv, \quad (3.24)$$

and considering the following ansatz for the scalar field

$$\varphi = \frac{1}{a(r)} \phi(v, r) Y(\Omega), \quad (3.25)$$

the Klein-Gordon equation (3.1), for a massless scalar field, yields

$$2\partial_v \partial_r \phi + f(r) \partial_r^2 \phi + f'(r) \partial_r \phi - 2iqA_v(r) \partial_r \phi - f'(r) \frac{a'(r)}{a(r)} \phi - iqA'_v(r) \phi - f(r) \frac{a''(r)}{a(r)} \phi - \frac{\kappa^2}{a(r)^2} \phi = 0. \quad (3.26)$$

Performing the change of variable $z = \frac{2r_+}{r} - 1$, the above equation becomes

$$\begin{aligned} & \partial_z \partial_v \phi - \frac{1}{4r_+} (1+z)^2 f(z) \partial_z^2 \phi - \left(\frac{1+z}{2r_+} f(z) + \frac{(1+z)^2}{4r_+} \frac{df}{dz} + iqA_v(z) \right) \partial_z \phi \\ & - \left(-\frac{1}{4r_+} (1+z)^2 \frac{df}{dz} \frac{1}{a} \frac{da}{dz} + \frac{iq}{2} \frac{dA_v}{dz} - \frac{f}{a} \left(\frac{1+z}{2r_+} \frac{da}{dz} + \frac{(1+z)^2}{4r_+} \frac{d^2 a}{dz^2} \right) - \frac{\kappa^2 r_+}{(1+z)^2 a^2} \right) \phi = 0. \end{aligned} \quad (3.27)$$

In the new coordinate the horizon is located at $z = 1$ and the spatial infinity at $z = -1$. Now, in order to solve the above differential equation we use the pseudospectral Chebyshev method, see for instance [52, 53]. The solution for the scalar field at any time is assumed to be a finite linear combination of the Chebyshev polynomials, with time dependent coefficients. Then, the solution is discretized at the Chebyshev collocation points, and the approximate solution is forced to satisfy the equation only at the Chebyshev collocation points. Furthermore, the exact derivatives are replaced by derivatives of interpolating polynomials at the Chebyshev points.

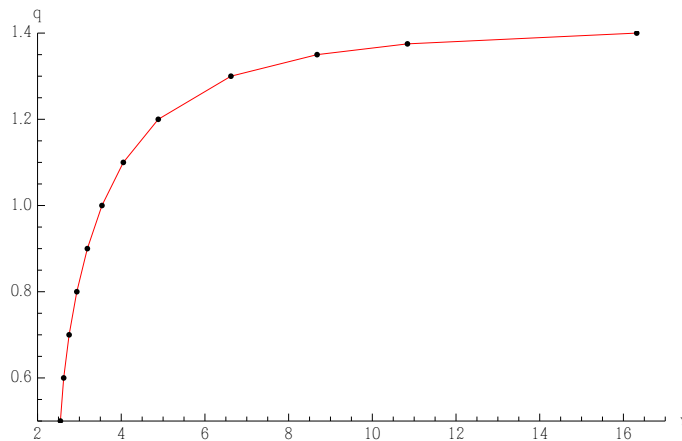


FIG. 5: Behaviour of q_c (red curve) versus ν for $\kappa = 0$, $\alpha_1 = 1$, $\alpha_2 = 2$, $\Lambda = -0.1$, $k = 1$ and $m = 0$. For $q > q_c$ the QNFs are unstable, for $q = q_c$ the QNFs have null imaginary part and for $q < q_c$ the QNFs are stable against radial massless charged scalar fields perturbations.

To integrate the system of differential equations in the time direction, we use the fourth order Runge-Kutta method. As initial condition for the scalar field we consider a Gaussian wave packet. Additionally, we set the boundary condition at spatial infinity as $\phi(v, z = -1) = 0$. In Fig. 6 we show the evolution of massless scalar field in time, we plot the logarithm of the absolute value of $\phi(v, r_0)$ vs v , for r_0 outside the horizon, and we can observe that the behaviour showed in the figures agrees with the results showed in Tables II and III. In fact, we can see that for $\nu = 5.5, 5$ the amplitude of the scalar field decreases in time which agrees with the results of the Tables because the imaginary part of the fundamental QNFs are negative in these cases. On the other hand, for $\nu = 4.53, 2.7, 2.511936559$ the amplitude of the scalar field grows in time and the Tables show that the imaginary part of the QNFs are positive, which is due to a superradiant instability as we will show in the next section. Besides, In Fig. 7, we show the evolution of massless scalar field in time in the background of a extremal black hole, for $\kappa = 0$, $\alpha_1 = 1$, $\alpha_2 = 2$, $\Lambda = -0.1$, $\nu = 2.511936559$, $k = 1$ and different values of q . We can observe that the amplitude of the scalar field grows in time, although, for smaller values of the q , the scalar field grows more slowly than for large values of q , which also will be showed be due to a superradiant instability.

Now, we use the time profile data obtained from the time domain integration to calculate the predominant QNF using the Prony method, which fits the profile data using a superposition of damping exponents, [51, 54, 55], in the following form

$$\phi(v, r) \approx \sum_{i=1}^p C_i e^{-i\omega_i(v-v_0)}. \quad (3.28)$$

In the above equation, we have considered that the quasinormal ringing epoch starts at $v = v_0$ and ends at $v = v_0 + Nh$, where h denotes the step size in the time direction and the integer $N \geq 2p - 1$. Formula (3.28) is valid for each value from the profile data so, one obtain a set of equations

$$x_n \equiv \phi(nh + v_0, r) = \sum_{j=1}^p C_j e^{-i\omega_j nh} = \sum_{j=1}^p C_j z_j^n. \quad (3.29)$$

The Prony method allows to find z_i in terms of known x_n and so, obtain the QNFs, which are given by the formula

$$w_j = \frac{i}{h} \ln(z_j). \quad (3.30)$$

In Table V we show some fundamental QNFs obtained by applying the Prony method to the time profile data, for $q = 1.2$, $\kappa = 0$, $\alpha_1 = 1$, $\alpha_2 = 2$, $\Lambda = -0.1$, $m = 0$, $k = 1$ and different values of ν . We see that the values are in good agreement with the values obtained from the improved AIM. The QNFs coincide up to four decimals with respect

to the improved AIM for the parameters considered. However with the time profile analysis we were able to obtain the QNFs for the near extremal and extremal black hole. Also, in Table VI we have calculated QNFs for a nearly extremal black hole ($\nu = 2.512$) and in Table VII for the extremal black hole ($\nu = 2.511936559$), for $\kappa = 0$, $\alpha_1 = 1$, $\alpha_2 = 2$, $\Lambda = -0.1$, $k = 1$, and different values of q . Note that for the nearly extremal black hole $\Delta r = 0.02$ and for the extremal black hole $\Delta r = 1.5 \cdot 10^{-8}$. We observe that the scalar perturbations on the extremal black holes are always unstable, due to the imaginary part of the QNFs which is positive, as Table VII shows. For $q = 0$ we see that the value of the QNF is approximately zero, and by increasing the number of collocation points from 50 to 90, we obtain $\omega = 4 \cdot 10^{-6}$ in this case which shows a convergence to zero as expected, see Fig. 8. Also, for $q = 1$ and 90 collocation points we obtain $\omega = 1.36584 + 0.01065i$ which is in good agreement with the value shown in Table VII. It is worth to mention that the values of Table VII agree with the observed in Fig. 7, that we have discussed previously.

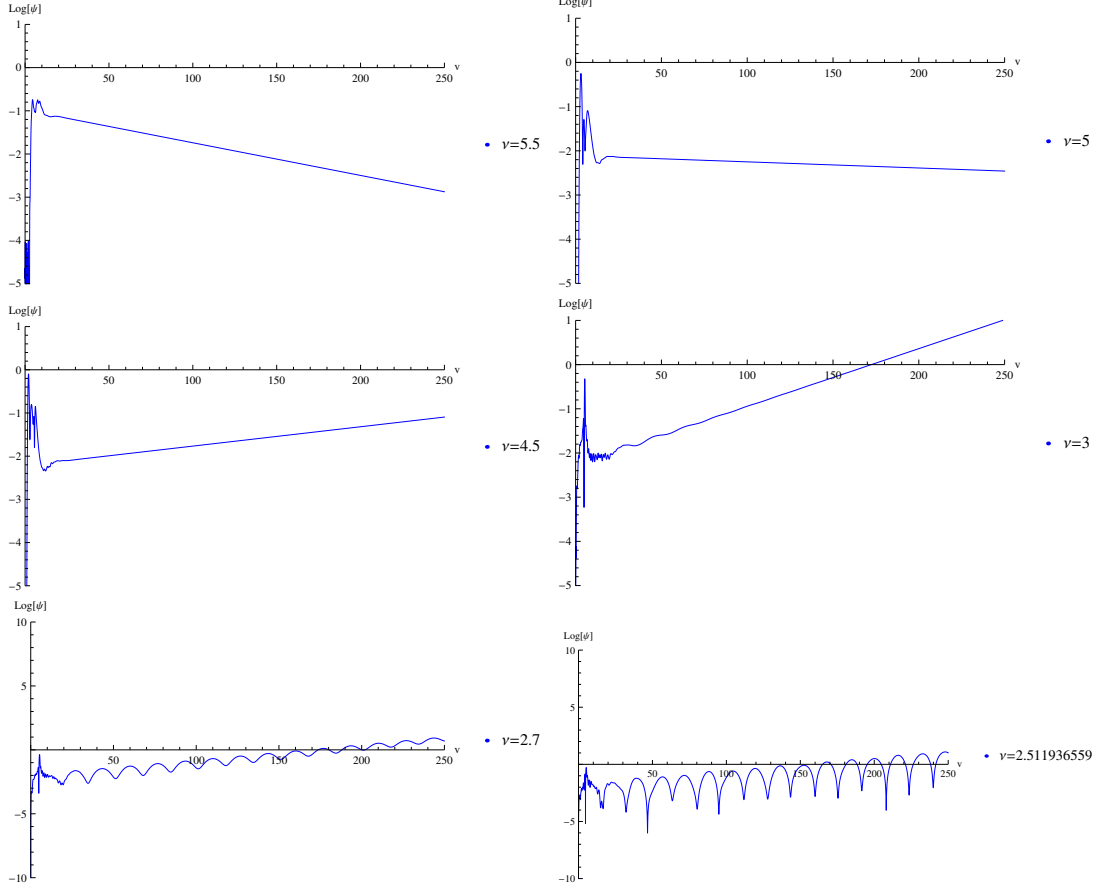


FIG. 6: Time evolution of charged massless scalar field for $\kappa = 0$, $\alpha_1 = 1$, $\alpha_2 = 2$, $\Lambda = -0.1$, $q = 1.2$, $k = 1$ and different values of ν .

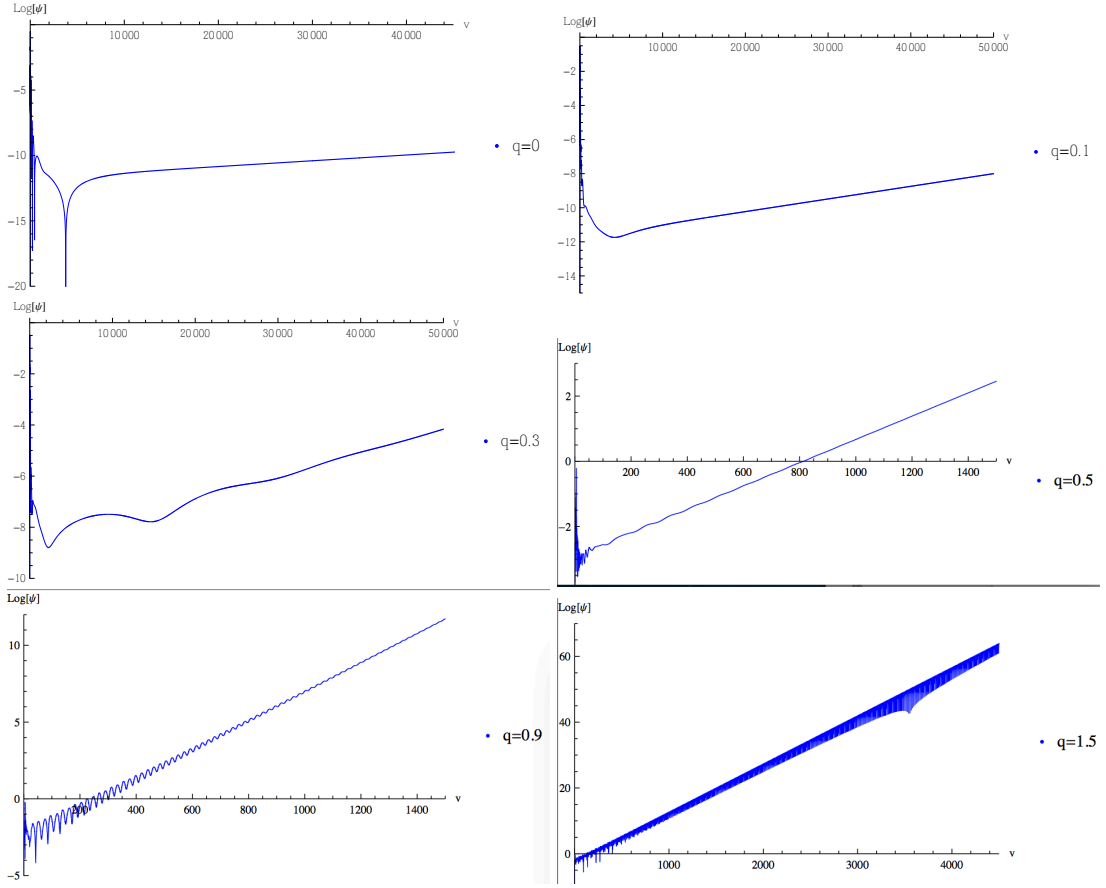


FIG. 7: Time evolution of charged massless scalar field for $\kappa = 0$, $\alpha_1 = 1$, $\alpha_2 = 2$, $\Lambda = -0.1$, $\nu = 2.511936559$ (Extremal case), $k = 1$ and different values of q .

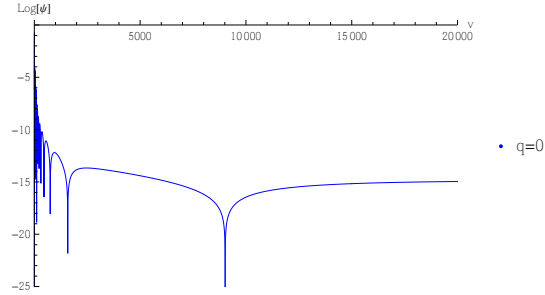


FIG. 8: Time evolution of charged massless scalar field for $\kappa = 0$, $\alpha_1 = 1$, $\alpha_2 = 2$, $\Lambda = -0.1$, $\nu = 2.511936559$ (Extremal case), $k = 1$, $q = 0$ and 90 collocation points.

Now having the QNFs from the time domain analysis we can improve the behaviour of the Fig. 4 that we have showed in the improved AIM section. So, in Fig. 9 we plot the behaviour of ω in the complex plane, by considering the transition from a hairy black hole to the extremal hairy black hole, and we can observe as the QNFs converge to the QNFs for the extremal case and that for some cases, when the QNFs have a positive imaginary part, the imaginary part present a maximum value and then decay, while that in other cases, for small values of the charge q , the imaginary part of the QNFs always increases.

TABLE V: Fundamental quasinormal frequencies for radial charged massless scalar fields in the background of the charged hairy black hole with $q = 1.2$, $\kappa = 0$, $\alpha_1 = 1$, $\alpha_2 = 2$, $\Lambda = -0.1$, $m = 0$, $k = 1$ and different values of ν .

ν	Δr	$q = 1.2$
5.50	7.48	$2.99238 - 0.00756i$
5.00	6.59	$2.73744 - 0.00139i$
4.50	5.66	$2.48457 + 0.00448i$
4.00	4.68	$2.23426 + 0.00944i$
3.50	3.61	$1.98657 + 0.01246i$
3.00	2.38	$1.74045 + 0.01308i$
2.70	1.41	$1.59341 + 0.01295i$
2.55	0.62	$1.52013 + 0.01289i$
2.511938	0.0038	$1.50119 + 0.01232i$
2.511936559	$1.5 \cdot 10^{-8}$	$1.50114 + 0.01239i$

TABLE VI: Fundamental quasinormal frequencies for charged massless scalar fields in the background of a nearly extremal charged hairy black hole with $\kappa = 0$, $\alpha_1 = 1$, $\alpha_2 = 2$, $\Lambda = -0.1$, $k = 1$, $\nu = 2.512$ and different values of q .

$q = 0.3$	$q = 0.35$	$q = 0.5$	$q = 0.9$	$q = 1$
$0.59376 - 0.00135i$	$0.68937 + 0.00029i$	$0.91333 + 0.00363i$	$1.29178 + 0.00987i$	$1.36537 + 0.01067i$

IV. SUPERRADIANT EFFECT

In this Section we will study the superradiant effect of a radial massive charged scalar field of the form (3.2) scattered off the horizon of the charged hairy black hole (2.17). In a pioneering work Bekenstein showed [42] that if the condition

$$\omega < q\Phi, \quad (4.1)$$

is satisfied, where q is the charge coupling constant of the field and Φ is the electric potential of the charged black hole, then the superradiant scattering of charged scalar field results in the extraction of Coulomb energy and electric charge from the charged black hole. Then, this amplification of charged massive fields by charged black holes leads to an instability of the Reissner-Nordström spacetime.

This charged radiation extracted from the event horizon of the black hole has to traverse a nontrivial, curved spacetime geometry before it eventually reaches asymptotic infinity. This radiation procedure if it takes place in an AdS space works as a potential barrier for the radiation, giving a deviation from the blackbody radiation spectrum and this deviation is measure by the greybody factor. To be able to measure this energy we have to trap these scattered waves in a cavity which usually is created by an effective potential outside the black hole horizon and then from the absorption and scattering cross sections of these waves compute their corresponding coefficients (for a recent review on superradiance see [56]).

To find the conditions for superradiance amplification of scatter wave we will compute the greybody factor and the reflection coefficients. Then if the greybody factor is negative or the reflection coefficients is greater than 1 [57] then the scalar waves can be superradiantly amplified by black hole. Following [58] we will split the spacetime in three regions and we will consider the low frequency limit, that is $\omega + qA_t(r_+) \ll T_H$ and $(\omega + qA_t(r_+))r_+ \ll 1$, and by simplicity we consider $\ell = 0$.

- Region I: The region near the event horizon, defined by $r \approx r_+$ and $V_{eff}(r) \approx -2q\omega A_t(r_+) - q^2 A_t(r_+)^2$ or $V_{eff}(r)|_{q=0} \ll (\omega + qA_t)^2$. In the first region, the solution to the radial equation is given by equation (3.14), that can be rewritten as

$$R(r) = A_I e^{-i(\omega + qA_t(r_+))r^*}, \quad (4.2)$$

which slightly away the horizon yields

$$R(r) = A_I \left(1 - \frac{i(\omega + qA_t(r_+))}{f'(r_+)} \log \left(\frac{r - r_+}{r_+} \right) \right). \quad (4.3)$$

TABLE VII: Fundamental quasinormal frequencies for charged massless scalar fields in the background of an extremal charged hairy black hole with $\kappa = 0$, $\alpha_1 = 1$, $\alpha_2 = 2$, $\Lambda = -0.1$, $k = 1$, $\nu = 2.511936559$ and different values of q .

$q = 0$	$q = 0.3$	$q = 0.35$	$q = 0.4$	$q = 0.45$
$0.00004i$	$0.59423 + 0.00009i$	$0.68973 + 0.00036i$	$0.77461 + 0.00134i$	$0.84821 + 0.00257i$
$q = 0.5$	$q = 0.9$	$q = 1$	$q = 1.2$	$q = 1.5$
$0.91326 + 0.00357i$	$1.29171 + 0.00948i$	$1.36536 + 0.01113i$	$1.50114 + 0.01239i$	$1.68163 + 0.01470i$

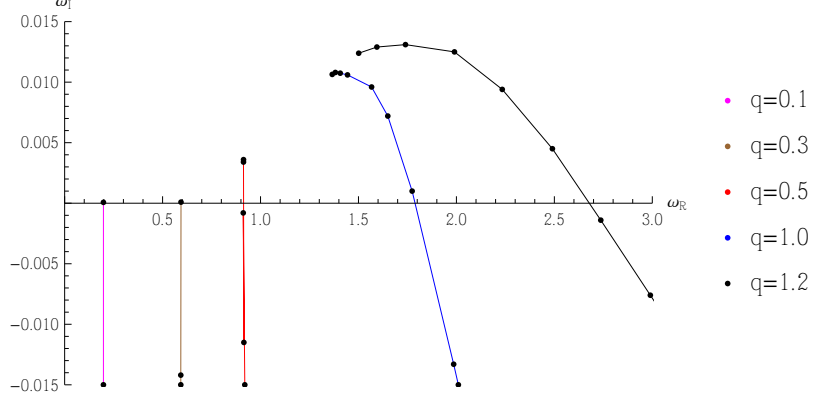


FIG. 9: The behavior of ω in the complex plane for $\kappa = 0$, $\alpha_1 = 1$, $\alpha_2 = 2$, $\Lambda = -0.1$, $m = 0$, $k = 1$ and different values of q and ν .

- Region II: The intermediate region, between the horizon region and the asymptotic region. This region is defined by $V_{eff}(r)|_{q=0} \gg (\omega + qA_t)^2$.

In this case the radial equation (3.3) reduces to

$$\frac{d}{dr} \left(a(r)^2 f(r) \frac{dR}{dr} \right) = 0, \quad (4.4)$$

whose solution is given by

$$R(r) = A_{II} + B_{II}G(r), \quad (4.5)$$

where

$$G(r) = \int_{\infty}^r \frac{dr}{f(r)a(r)^2}. \quad (4.6)$$

So, for $r \approx r_+$ we obtain

$$G(r) \approx \frac{1}{f'(r_+)r_+(r_+ + \nu)} \log \left(\frac{r - r_+}{r_+} \right). \quad (4.7)$$

Matching this solution with the solution of region I, we obtain

$$A_{II} = A_I, \quad B_{II} = -i(\omega + qA_t(r_+))r_+(r_+ + \nu)A_I. \quad (4.8)$$

On the other hand, for $r \gg r_+$

$$G(r) \approx \int_{\infty}^r \frac{dr}{-\frac{\Lambda r^2}{3}a(r)^2} = -\frac{1}{\Lambda r^3}. \quad (4.9)$$

Therefore

$$R(r) = A_I \left(1 - \frac{i(\omega + qA_t(r_+))r_+(r_+ + \nu)}{\Lambda r^3} \right), \quad (4.10)$$

which will be matched with asymptotic behaviour.

- Region III: The asymptotic region. This region is defined by $r \gg r_+$.

In this case, for our purposes it is enough to take into account just the leading term in the asymptotic behaviour of the effective potential, which is given by

$$V_{eff}(r) \approx \frac{2\Lambda^2 r^2}{9}, \quad (4.11)$$

and the tortoise coordinate at infinity is given by

$$r^* = \frac{2}{\sqrt{4 + \Lambda\nu^2/3}\sqrt{-\Lambda/3}} \arctan\left(\frac{(2r + \nu)\sqrt{-\Lambda/3}}{\sqrt{4 + \Lambda\nu^2/3}}\right). \quad (4.12)$$

In this way, the solution of the radial equation in the asymptotic region is

$$R(r) = C_1 + C_2/r^3. \quad (4.13)$$

Then, matching the solution of region II, for $r \gg r_+$, with the solution of region III yields

$$C_1 = A_I, \quad C_2 = -i(\omega + qA_t(r_+))r_+(r_+ + \nu)A_I/\Lambda. \quad (4.14)$$

Now, we will compute the fluxes, that are given by the following expression

$$\mathcal{F} = \frac{\sqrt{-g}g^{rr}}{2i} (R^* \partial_r R - R \partial_r R^*). \quad (4.15)$$

So, at the horizon we have

$$\mathcal{F}_{hor} \propto -(\omega + qA_t(r_+))r_+(r_+ + \nu)|A_I|^2. \quad (4.16)$$

and at infinity by

$$\mathcal{F}_\infty \propto -\Lambda \text{Im}(C_1 C_2^*). \quad (4.17)$$

In order to characterize the fluxes at the asymptotic region, is convenient to split up the coefficients C_1 and C_2 in terms of the incoming and outgoing coefficients, \hat{C}_2 and \hat{C}_1 , respectively. We define $C_1 = \hat{C}_1 + \hat{C}_2$ and $C_2 = i(\hat{C}_2 - \hat{C}_1)$. Therefore, the asymptotic incoming and outgoing fluxes are given by

$$\mathcal{F}_{in \infty} \propto \Lambda |\hat{C}_2|^2 = \Lambda \frac{|A_I|^2}{4} \left(1 - \frac{(\omega + qA_t(r_+))r_+(r_+ + \nu)}{\Lambda}\right)^2, \quad (4.18)$$

$$\mathcal{F}_{out \infty} \propto -\Lambda |\hat{C}_1|^2 = -\Lambda \frac{|A_I|^2}{4} \left(1 + \frac{(\omega + qA_t(r_+))r_+(r_+ + \nu)}{\Lambda}\right)^2. \quad (4.19)$$

Then, the reflection coefficient and the greybody factor [58–65] yields

$$\mathcal{R} = \frac{\mathcal{F}_{out \infty}}{\mathcal{F}_{in \infty}} = \left(\frac{1 + \frac{(\omega + qA_t(r_+))r_+(r_+ + \nu)}{\Lambda}}{1 - \frac{(\omega + qA_t(r_+))r_+(r_+ + \nu)}{\Lambda}}\right)^2, \quad (4.20)$$

$$\gamma(\omega) = \frac{\mathcal{F}_{hor}}{\mathcal{F}_{in \infty}} = \frac{-4(\omega + qA_t(r_+))r_+(r_+ + \nu)}{\left(1 - \frac{(\omega + qA_t(r_+))r_+(r_+ + \nu)}{\Lambda}\right)^2}. \quad (4.21)$$

Finally, it is possible to find the superradiant condition from the reflection coefficient or from the greybody factor. So the reflection coefficient is greater than 1 or alternatively the greybody factor is negative if $\omega + qA_t(r_+) < 0$ or

$$\omega < q\sqrt{\alpha_1}\nu \log(1 + \nu/r_+). \quad (4.22)$$

Note that this condition because the parameter of the scalar field ν is related to the charge Q of the black hole (relation (2.15)), modifies the Bekenstein's superradiance condition (4.1) introducing the information of the presence of the scalar hair. The analysis was performed for the non-extremal case; however, the same condition (4.22) still holds for the extremal black hole. Then the comparison of the real part of the dominant modes, that we have found in the previous section, with the superradiant condition of charged scalar fields [66–72] suggests that all the unstable modes are superradiant unstable and consequently the scalar waves can be superradiantly amplified by the black hole.

V. CONCLUSIONS

We have studied the QNFs of radial scalar field perturbations of near extremal and extremal four-dimensional charged hairy black holes in AdS spacetime. First, we have studied the case of hairy black hole by using the improved AIM and we have found the fundamental QNFs for radial neutral scalar field perturbations. In this case, for all cases analyzed, we have showed that the system is overdamped, that is the QNFs have no real part so there is no oscillatory behaviour in the perturbations, only exponential decay. Moreover, the imaginary part of the QNFs is negative, which guarantees the stability of the propagation of massive neutral scalar fields in such background. However, when the distance between the two roots of the lapsus function decreases, it is more difficult to find the QNFs by using the improved AIM. So, in order to obtain the QNFs for the near extremal and extremal black hole, we have applied the time domain analysis. In general, for the cases analyzed, we have showed that the QNFs of the near extremal black hole converge to the QNFs for the extremal black hole.

When we considered the propagation of massless charged scalar fields we have found that the QNFs present real and imaginary parts, even in some cases the imaginary part is positive, which indicates that the propagation of charged massless scalar fields is unstable. Then, we have studied the superradiance effect calculating the superradiant condition. We have found that the superradiant condition depends on ν , the charge of the scalar field that backreacts on the geometry, giving hair to the charged black hole. The presence of ν in the superradiant condition, which is proportional to Q the charge of the hairy black hole, modifies in a non-trivial way the Bekenstein's superradiance condition. We have also found that the critical value of the charged scalar perturbations q_c giving unstable modes, is related to the charge of the scalar hair ν and there is a maximum value of ν which can trigger the superradiant instability. Finally, we have found that all the unstable modes are superradiant and all the stable modes are not superradiant, satisfying the superradiant condition, and consequently the radial scalar waves can be superradiantly amplified by black hole by extracting charged of the black hole which indicates that the black hole is unstable.

It is worth mentioning that it would be interesting to analyze the superradiant instability of this hairy black hole for charged massive scalar field with non vanishing angular momentum, due to the fact that in some cases the instability is sensitive to the parity of the orbital quantum number (for instance see [68]), which we left for a future work.

Acknowledgments

We thank Emanuelle Berti and Bin Wang for their useful comments and remarks. This work was partially funded by Comisión Nacional de Ciencias y Tecnología through FONDECYT Grants 11140674 (PAG) and by the Dirección de Investigación y Desarrollo de la Universidad de La Serena (Y.V.). P. A. G. acknowledges the hospitality of the Universidad de La Serena, National Technical University of Athens and Pontificia Universidad Católica de Valparaíso, E. P. acknowledges the hospitality of the Universidad Diego Portales and Pontificia Universidad Católica de Valparaíso and Y. V. acknowledges the hospitality of the Pontificia Universidad Católica de Valparaíso where part of this work was undertaken.

Appendix A: Improved AIM

In this appendix we give a brief review of the improved AIM, which is used to solve homogeneous linear second-order differential equations subject to boundary conditions. First, it is necessary to implement the boundary conditions. For this purpose the dependent variable must be redefined in terms of a new function, say χ , that satisfies the boundary conditions appropriate to the eigenvalue problem under consideration. Thus, in order to implement the improved AIM the differential equation must be written in the form

$$\chi'' = \lambda_0(y)\chi' + s_0(y)\chi. \quad (\text{A1})$$

Then, one must differentiate Eq. (A1) n times with respect to y , which yields the following equation:

$$\chi^{n+2} = \lambda_n(y)\chi' + s_n(y)\chi, \quad (\text{A2})$$

where

$$\lambda_n(y) = \lambda'_{n-1}(y) + s_{n-1}(y) + \lambda_0(y)\lambda_{n-1}(y), \quad (\text{A3})$$

$$s_n(y) = s'_{n-1}(y) + s_0(y)\lambda_{n-1}(y). \quad (\text{A4})$$

Then, expanding the λ_n and s_n in a Taylor series around some point η , at which the improved AIM is performed, yields

$$\lambda_n(\eta) = \sum_{i=0}^{\infty} c_n^i (y - \eta)^i, \quad (\text{A5})$$

$$s_n(\eta) = \sum_{i=0}^{\infty} d_n^i (y - \eta)^i, \quad (\text{A6})$$

where the c_n^i and d_n^i are the i^{th} Taylor coefficients of $\lambda_n(\eta)$ and $s_n(\eta)$, respectively, and by replacing the above expansions in Eqs. (A3) and (A4) the following set of recursion relations for the coefficients is obtained

$$c_n^i = (i+1)c_{n-1}^{i+1} + d_{n-1}^i + \sum_{k=0}^i c_0^k c_{n-1}^{i-k}, \quad (\text{A7})$$

$$d_n^i = (i+1)d_{n-1}^{i+1} + \sum_{k=0}^i d_0^k c_{n-1}^{i-k}. \quad (\text{A8})$$

In this manner, the authors of the improved AIM have avoided the derivatives that contain the AIM in [29, 36], and the quantization condition, which is equivalent to imposing a termination to the number of iterations, is given by

$$d_n^0 c_{n-1}^0 - d_{n-1}^0 c_n^0 = 0. \quad (\text{A9})$$

- [1] T. Regge and J.A. Wheeler, Stability of a Schwarzschild singularity, *Phys. Rev.* **108** (1957) 1063.
- [2] F. J. Zerilli, “Gravitational field of a particle falling in a schwarzschild geometry analyzed in tensor harmonics,” *Phys. Rev. D* **2**, 2141 (1970).
- [3] F. J. Zerilli, “Effective potential for even parity Regge-Wheeler gravitational perturbation equations,” *Phys. Rev. Lett.* **24**, 737 (1970).
- [4] K. D. Kokkotas and B. G. Schmidt, “Quasinormal modes of stars and black holes,” *Living Rev. Rel.* **2**, 2 (1999) [gr-qc/9909058].
- [5] H. -P. Nollert, “TOPICAL REVIEW: Quasinormal modes: the characteristic ‘sound’ of black holes and neutron stars,” *Class. Quant. Grav.* **16**, R159 (1999).
- [6] E. Berti, “Black hole quasinormal modes: Hints of quantum gravity?,” *Conf. Proc. C* **0405132**, 145 (2004) [gr-qc/0411025].
- [7] R. A. Konoplya and A. Zhidenko, “Quasinormal modes of black holes: From astrophysics to string theory,” *Rev. Mod. Phys.* **83**, 793 (2011), [arXiv:1102.4014 [gr-qc]].
- [8] P. R. Brady, C. M. Chambers, W. Krivan and P. Laguna, “Telling tails in the presence of a cosmological constant,” *Phys. Rev. D* **55**, 7538 (1997) [gr-qc/9611056]; P. R. Brady, C. M. Chambers, W. G. Laarakkers and E. Poisson, “Radiative falloff in Schwarzschild-de Sitter space-time,” *Phys. Rev. D* **60**, 064003 (1999) [gr-qc/9902010]; T. R. Choudhury and T. Padmanabhan, “Quasinormal modes in Schwarzschild-deSitter space-time: A Simple derivation of the level spacing of the frequencies,” *Phys. Rev. D* **69**, 064033 (2004) [gr-qc/0311064]; D. P. Du, B. Wang and R. K. Su, “Quasinormal modes in pure de Sitter space-times,” *Phys. Rev. D* **70**, 064024 (2004) [hep-th/0404047].
- [9] C. Molina, “Quasinormal modes of d-dimensional spherical black holes with near extreme cosmological constant,” *Phys. Rev. D* **68**, 064007 (2003) [gr-qc/0304053]; C. Molina, D. Giugno, E. Abdalla and A. Saa, “Field propagation in de Sitter black holes,” *Phys. Rev. D* **69**, 104013 (2004) [gr-qc/0309079].
- [10] J. S. F. Chan and R. B. Mann, “Scalar wave falloff in asymptotically anti-de Sitter backgrounds,” *Phys. Rev. D* **55**, 7546 (1997) [gr-qc/9612026]; J. S. F. Chan and R. B. Mann, “Scalar wave falloff in topological black hole backgrounds,” *Phys. Rev. D* **59**, 064025 (1999).
- [11] G. T. Horowitz and V. E. Hubeny, “Quasinormal modes of AdS black holes and the approach to thermal equilibrium,” *Phys. Rev. D* **62**, 024027 (2000) [hep-th/9909056].
- [12] B. Wang, C. Y. Lin and E. Abdalla, “Quasinormal modes of Reissner-Nordstrom anti-de Sitter black holes,” *Phys. Lett. B* **481**, 79 (2000) [hep-th/0003295].
- [13] B. Wang, C. Molina and E. Abdalla, “Evolving of a massless scalar field in Reissner-Nordstrom Anti-de Sitter space-times,” *Phys. Rev. D* **63**, 084001 (2001) [hep-th/0005143].
- [14] S. S. Gubser, “Phase transitions near black hole horizons,” *Class. Quant. Grav.* **22**, 5121 (2005) [hep-th/0505189].

- [15] S. S. Gubser, “Breaking an Abelian gauge symmetry near a black hole horizon,” *Phys. Rev. D* **78**, 065034 (2008) [arXiv:0801.2977 [hep-th]].
- [16] S. A. Hartnoll, C. P. Herzog, and G. T. Horowitz, “Building a Holographic Superconductor,” *Phys.Rev.Lett.* **101** (2008) 031601, [arXiv:0803.3295 [hep-th]]
- [17] X. M. Kuang and E. Papantonopoulos, “Building a Holographic Superconductor with a Scalar Field Coupled Kinematically to Einstein Tensor,” *JHEP* **1608**, 161 (2016) [arXiv:1607.04928 [hep-th]].
- [18] G. T. Horowitz and M. M. Roberts, “Zero Temperature Limit of Holographic Superconductors,” *JHEP* **0911**, 015 (2009,) [arXiv:0908.3677 [hep-th]].
- [19] A. Chamblin, R. Emparan, C. V. Johnson and R. C. Myers, “Charged AdS black holes and catastrophic holography,” *Phys. Rev. D* **60**, 064018 (1999) arXiv:hep-th/9902170.
- [20] H. K. Kunduri and J. Lucietti, “Classification of near-horizon geometries of extremal black holes,” *Living Rev. Rel.* **16**, 8 (2013) [arXiv:1306.2517 [hep-th]].
- [21] E. Berti and K. D. Kokkotas, “Quasinormal modes of Reissner-Nordstrom-anti-de Sitter black holes: Scalar, electromagnetic and gravitational perturbations,” *Phys. Rev. D* **67**, 064020 (2003) [gr-qc/0301052].
- [22] S. Mahapatra, *JHEP* **1604**, 142 (2016) doi:10.1007/JHEP04(2016)142 [arXiv:1602.03007 [hep-th]].
- [23] H. Onozawa, T. Mishima, T. Okamura and H. Ishihara, “Quasinormal modes of maximally charged black holes,” *Phys. Rev. D* **53**, 7033 (1996) [gr-qc/9603021].
- [24] M. Richartz, “Quasinormal modes of extremal black holes,” *Phys. Rev. D* **93**, no. 6, 064062 (2016), [arXiv:1509.04260 [gr-qc]].
- [25] P. A. Gonzalez, E. Papantonopoulos, J. Saavedra and Y. Vasquez, “Extremal Hairy Black Holes,” *JHEP* **1411**, 011 (2014) [arXiv:1408.7009 [gr-qc]].
- [26] J. Barrientos, P. A. Gonzalez and Y. Vasquez, “Four-dimensional black holes with scalar hair in nonlinear electrodynamics,” *Eur. Phys. J. C* **76**, no. 12, 677 (2016) [arXiv:1603.05571 [hep-th]].
- [27] P. A. Gonzalez, E. Papantonopoulos, J. Saavedra and Y. Vasquez, “Four-Dimensional Asymptotically AdS Black Holes with Scalar Hair,” *JHEP* **1312**, 021 (2013), [arXiv:1309.2161 [gr-qc]].
- [28] O. J. C. Dias and R. Masachs, “Hairy black holes and the endpoint of AdS₄ charged superradiance,” arXiv:1610.03496 [hep-th].
- [29] H. T. Cho, A. S. Cornell, J. Doukas and W. Naylor, “Black hole quasinormal modes using the asymptotic iteration method,” *Class. Quant. Grav.* **27** (2010) 155004 [arXiv:0912.2740 [gr-qc]].
- [30] H. Ciftci, R. L. Hall, and N. Saad, “Asymptotic iteration method for eigenvalue problems,” *J. Phys. A* **36**(47), 11807-11816 (2003).
- [31] H. Ciftci, R. L. Hall and N. Saad, “Perturbation theory in a framework of iteration methods,” *Phys. Lett. A* **340** (2005) 388.
- [32] G. Koutsoumbas, S. Musiri, E. Papantonopoulos and G. Siopsis, “Quasi-normal Modes of Electromagnetic Perturbations of Four-Dimensional Topological Black Holes with Scalar Hair,” *JHEP* **0610**, 006 (2006), [hep-th/0606096].
- [33] P. A. Gonzalez and Y. Vasquez, “Scalar Perturbations of Nonlinear Charged Lifshitz Black Branes with Hyperscaling Violation,” *Astrophys. Space Sci.* **361**, no. 7, 224 (2016) [arXiv:1509.00802 [hep-th]].
- [34] R. Becar, P. A. Gonzalez and Y. Vasquez, “Quasinormal modes of non-Abelian hyperscaling violating Lifshitz black holes,” arXiv:1510.04605 [hep-th].
- [35] R. Becar, P. A. Gonzalez and Y. Vasquez, “Quasinormal modes of Four Dimensional Topological Nonlinear Charged Lifshitz Black Holes,” *Eur. Phys. J. C* **76**, no. 2, 78 (2016) [arXiv:1510.06012 [gr-qc]].
- [36] H. T. Cho, A. S. Cornell, J. Doukas, T. R. Huang and W. Naylor, “A New Approach to Black Hole Quasinormal Modes: A Review of the Asymptotic Iteration Method,” *Adv. Math. Phys.* **2012** (2012) 281705 [arXiv:1111.5024 [gr-qc]].
- [37] M. Catalan, E. Cisternas, P. A. Gonzalez and Y. Vasquez, “Dirac quasinormal modes for a 4-dimensional Lifshitz black hole,” *Eur. Phys. J. C* **74** (2014) 3, 2813 [arXiv:1312.6451 [gr-qc]].
- [38] M. Catalan, E. Cisternas, P. A. Gonzalez and Y. Vasquez, “Quasinormal modes and greybody factors of a four-dimensional Lifshitz black hole with $z=0$,” arXiv:1404.3172 [gr-qc].
- [39] W. Sybesma and S. Vandoren, “Lifshitz quasinormal modes and relaxation from holography,” *JHEP* **1505**, 021 (2015) [arXiv:1503.07457 [hep-th]].
- [40] C. Y. Zhang, S. J. Zhang and B. Wang, “Charged Scalar Perturbations around Garfinkle-Horowitz-Strominger Black Holes,” arXiv:1501.03260 [hep-th].
- [41] T. Barakat, “The asymptotic iteration method for Dirac and Klein-Gordon equations with a linear scalar potential,” *Int. J. Mod. Phys. A* **21** (2006) 4127.
- [42] J. D. Bekenstein, “Extraction of energy and charge from a black hole,” *Phys. Rev. D* **7**, 949 (1973).
- [43] P. Breitenlohner and D. Z. Freedman, “Stability In Gauged Extended Supergravity,” *Annals Phys.* **144**, 249 (1982).
- [44] G. Koutsoumbas, E. Papantonopoulos and G. Siopsis, “Exact Gravity Dual of a Gapless Superconductor,” *JHEP* **0907**, 026 (2009), [arXiv:0902.0733 [hep-th]].
- [45] P. A. Gonzalez, M. Olivares and Y. Vasquez, “Motion of particles on a Four-Dimensional Asymptotically AdS Black Hole with Scalar Hair,” *Eur. Phys. J. C* **75**, no. 10, 464 (2015) [arXiv:1507.03610 [gr-qc]].
- [46] D. Garfinkle and L. A. Pando Zayas, “Rapid Thermalization in Field Theory from Gravitational Collapse,” *Phys. Rev. D* **84**, 066006 (2011) [arXiv:1106.2339 [hep-th]].
- [47] D. Garfinkle, L. A. Pando Zayas and D. Reichmann, “On Field Theory Thermalization from Gravitational Collapse,” *JHEP* **1202**, 119 (2012) [arXiv:1110.5823 [hep-th]].
- [48] B. Wang, C. Y. Lin and E. Abdalla, “Quasinormal modes of Reissner-Nordstrom anti-de Sitter black holes,” *Phys. Lett.*

- B **481**, 79 (2000) [hep-th/0003295].
- [49] J. Crisostomo, S. Lepe and J. Saavedra, *Class. Quant. Grav.* **21**, 2801 (2004) [hep-th/0402048].
- [50] R. Li, Y. Tian, H. b. Zhang and J. Zhao, “Time domain analysis of superradiant instability for the charged stringy black hole/mirror system,” *Phys. Lett. B* **750**, 520 (2015) [arXiv:1506.04267 [gr-qc]].
- [51] R. Li, H. Zhang and J. Zhao, “Time evolutions of scalar field perturbations in D-dimensional Reissner-Nordstrom Anti-de Sitter black holes,” *Phys. Lett. B* **758**, 359 (2016) [arXiv:1604.01267 [gr-qc]].
- [52] Y. Liu, The pseudospectral Chebyshev method for two-point boundary value problems, M.Sc. thesis, Department of Mathematics and Statistics, Simon Fraser University, Burnaby, B.C., Canada, 1992.
- [53] O. J. C. Dias, J. E. Santos and B. Way, “Numerical Methods for Finding Stationary Gravitational Solutions,” *Class. Quant. Grav.* **33**, no. 13, 133001 (2016) [arXiv:1510.02804 [hep-th]].
- [54] E. Berti, V. Cardoso, J. A. Gonzalez and U. Sperhake, “Mining information from binary black hole mergers: A Comparison of estimation methods for complex exponentials in noise,” *Phys. Rev. D* **75**, 124017 (2007) [gr-qc/0701086].
- [55] A. Zhidenko, “Linear perturbations of black holes: stability, quasi-normal modes and tails,” arXiv:0903.3555 [gr-qc].
- [56] R. Brito, V. Cardoso and P. Pani, “Superradiance : Energy Extraction, Black-Hole Bombs and Implications for Astrophysics and Particle Physics,” *Lect. Notes Phys.* **906**, pp.1 (2015) [arXiv:1501.06570 [gr-qc]].
- [57] C. L. Benone and L. C. B. Crispino, “Superradiance in static black hole spacetimes,” *Phys. Rev. D* **93**, no. 2, 024028 (2016) [arXiv:1511.02634 [gr-qc]].
- [58] T. Harmark, J. Natario and R. Schiappa, “Greybody Factors for d-Dimensional Black Holes,” *Adv. Theor. Math. Phys.* **14**, no. 3, 727 (2010) [arXiv:0708.0017 [hep-th]].
- [59] D. Birmingham, I. Sachs and S. Sen, “Three-dimensional black holes and string theory,” *Phys. Lett. B* **413** (1997) 281 [hep-th/9707188].
- [60] W. T. Kim and J. J. Oh, “Dilaton driven Hawking radiation in AdS(2) black hole,” *Phys. Lett. B* **461** (1999) 189 [hep-th/9905007].
- [61] J. J. Oh and W. Kim, “Absorption Cross Section in Warped AdS(3) Black Hole,” *JHEP* **0901** (2009) 067 [arXiv:0811.2632 [hep-th]].
- [62] H. C. Kao and W. Y. Wen, “Absorption cross section in warped AdS(3) black hole revisited,” *JHEP* **0909** (2009) 102 [arXiv:0907.5555 [hep-th]].
- [63] C. Campuzano, P. Gonzalez, E. Rojas and J. Saavedra, “Greybody factors for topological massless black holes,” *JHEP* **1006**, 103 (2010) [arXiv:1003.2753 [gr-qc]].
- [64] P. Gonzalez, E. Papantonopoulos and J. Saavedra, “Chern-Simons black holes: scalar perturbations, mass and area spectrum and greybody factors,” *JHEP* **1008** (2010) 050 [arXiv:1003.1381 [hep-th]].
- [65] P. A. Gonzalez and J. Saavedra, *Int. J. Mod. Phys. A* **26**, 3997 (2011) [arXiv:1104.4795 [gr-qc]].
- [66] V. Cardoso and O. J. C. Dias, “Small Kerr-anti-de Sitter black holes are unstable,” *Phys. Rev. D* **70**, 084011 (2004) [hep-th/0405006].
- [67] V. Cardoso, O. J. C. Dias and S. Yoshida, “Classical instability of Kerr-AdS black holes and the issue of final state,” *Phys. Rev. D* **74**, 044008 (2006) [hep-th/0607162].
- [68] A. N. Aliev and O. Delice, “Superradiant Instability of Five-Dimensional Rotating Charged AdS Black Holes,” *Phys. Rev. D* **79**, 024013 (2009) [arXiv:0808.0280 [hep-th]].
- [69] O. J. C. Dias, G. T. Horowitz and J. E. Santos, “Black holes with only one Killing field,” *JHEP* **1107**, 115 (2011) [arXiv:1105.4167 [hep-th]].
- [70] R. Li, “Superradiant instability of charged massive scalar field in Kerr-Newman-anti-de Sitter black hole,” *Phys. Lett. B* **714**, 337 (2012) [arXiv:1205.3929 [gr-qc]].
- [71] N. Uchikata and S. Yoshida, “Quasinormal modes of a massless charged scalar field on a small Reissner-Nordstrom-anti-de Sitter black hole,” *Phys. Rev. D* **83**, 064020 (2011) [arXiv:1109.6737 [gr-qc]].
- [72] V. Cardoso, O. J. C. Dias, G. S. Hartnett, L. Lehner and J. E. Santos, “Holographic thermalization, quasinormal modes and superradiance in Kerr-AdS,” *JHEP* **1404**, 183 (2014) [arXiv:1312.5323 [hep-th]].